Influence of edge surface quality on Hybrid Laser-Arc Welding of structural steel S355J2

Martin Petreski[a], Dobre Runchev[a], Gligorche Vrtanoski[a], Aleksandra Krstevska[a]

University „Ss. Cyril and Methodius“ in Skopje, Faculty of Mechanical Engineering – Skopje, Rugjer Boshkovikj 18, P.O. Box 464, MK-1000 Skopje[a]

martin.petreski@mf.edu.mk[a], dobre.runchev@mf.edu.mk[a], gligorche.vrtanoski@mf.edu.mk[a], aleksandra.krstevska@mf.edu.mk[a]

Abstract

Although hybrid laser-arc welding has several advantages over conventional welding processes, this process has certain limitations, such as small gap tolerances and misalignment of the edges due to the focus of the laser beam. It is common practice to perform edge preparation by milling to achieve greater accuracy in weld joint preparation, resulting in increased process efficiency and acceptable weld quality. Edge preparation by milling leads to higher costs and is sometimes inconvenient for the overall process, especially for material with a thickness higher than 8 mm. This study investigates the impact of the edge surface quality on the weld characteristics produced by hybrid laser-arc welding of 12-mm thick structural steel plates. Two different surface qualities were obtained by different industrial methods, plasma cutting and milling. Single-pass hybrid laser-arc welds were performed in a butt joint configuration with zero-gap by using the same process parameters, a laser beam power of 10 kW, welding speed 1.8 m min-1, welding current 355 A and arc voltage 36.8 V. Before welding the edge surface roughness values and roughness patterns were measured transversely and longitudinally, and tack welds at the beginning and end of the plates were applied to ensure the zero-gap and alignment of the edges. The weld characteristics were evaluated in terms of weld bead geometry and mechanical properties, tensile strength, and hardness. The results showed that edge surface quality impacts the choice of process parameters, weld quality, and process efficiency.

Keywords:
Edge surface quality, hybrid laser-arc welding, plasma cutting, milling, zero-gap, welding process parameters

1. Introduction

Hybrid laser-arc welding - HLAW is a productive welding process that combines the precision of laser beam welding and the robustness of arc welding, tailored for thick-section steels [1]. By coupling the synergy effects of both welding processes, the HLAW offers promising solutions to the challenges faced by conventional welding processes, especially in achieving deep penetration and high-quality welds in thick-section steels. The main advantages of this process lie in high welding speed, low heat input, minimal distortion, high penetration deep, and the possibility of controlling the chemical composition of the weld bead [1]. Despite all the advantages, the process has certain limitations, higher equipment costs, and controlling a number of welding parameters with their proper setting to prevent defects and avoid solidification cracks when it comes to welding thick-section steel [2]. Moreover, the efficiency of HLAW depends not only on the welding process parameters and their synchronization but also on the edge preparation method.

Various methods, such as machining, plasma or laser cutting, milling, grinding, etc., can significantly determine the weld's overall process efficiency and quality of the weld [3]. However, there is no correlation between the cut quality and weld quality in terms of the number of solidification cracks in the welds, but cut quality can determine the selection of the values of the process parameters [4].

According to Bunaziv et al. [11], the frame of process parameters selection was much more comprehensive for machined edges compared with plasma-cut edges in terms of process stability and root humping effect. On the other hand, the plasma-cut surface requires less laser power for welding, because the plasma-cut strips locally increase the joint gap [14]. Additionally, the natural gap in plasma-cut samples leads to 60% more filler material and the possibility of humping during single-pass HLAW thick structural steel plate. According to Üstündağ et al. [14] the surface roughness is directly to weld bead geometry and its mechanical properties in HLAW of thick-section steels. The combination of a pre-set air gap and a higher surface roughness can increase the weld penetration in thick low alloyed steel in the butt joint configuration. [14]. However, only a few studies have been published regarding the influence of cut surface quality on the HLAW process of thick-section steel, and more information is still needed about the effects of surface roughness on weld quality and the selection of process parameters.

The aim of this study is to investigate the influence of edge surface quality on the single–pass hybrid laser-arc weld of 12-mm thick structural steel. Several experiments were conducted using plasma cutting and milling edge surface preparation. Prior to welding, the surface quality was measured transversely and longitudinally, and tack welds ensured a zero-gap joint at the beginning and end of the plates. After the welding, visual inspection and mechanical tests, such as bending, tensile, and hardness tests, were performed. The final quality of the hybrid laser-arc welds was compared between the plasma-cut and milling edge preparation, and a conclusion was drawn on how the edge surface roughness affects process parameters and process efficiency.

2. Materials and methods

The welding experiments of the present study were conducted on 12 mm thick plates of structural steel in quality S355J2. The pieces were cut to dimensions 150 x 400 mm before welding preparation. The welds were performed in an I-joint configuration with zero-gap. The welding wire used for HLAW was a solid wire G3Ni1 according to EN ISO 14341-A: G 42 3 M21 3Si1 with a diameter of 1.2 mm. The materials' chemical composition and mechanical properties are shown in Table 1 and Table 2, respectively. As a shielding gas is used a mixture of argon with 18% CO2 – CORGON 18 according to EN ISO14175: M21 ArC 18 with a flow rate of 25 l min-1. The base material has a carbon equivalent value of max. 0.39 (CE_{IIW} for low alloy steels, CE_{IIW} = C + mn/6 + (Cr + Mo + V)/5 + (Cu + Ni)/15)

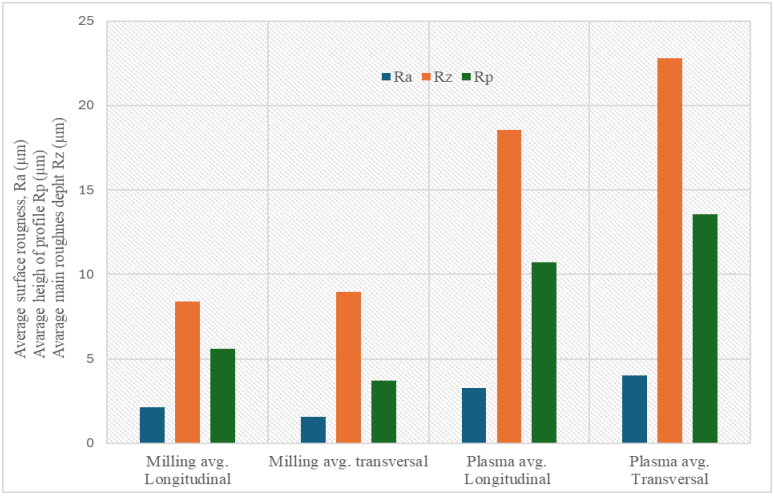

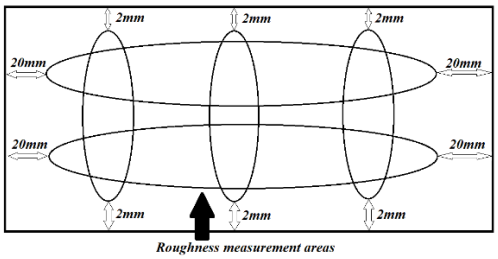

Fig 1. Results of surface roughness measurement

2.2 Surface preparation and measuring

Two different industrial methods were employed for edge preparation: milling and plasma cutting. The milling is performed on a CNC machining centre with a cutting speed of 90 m/min and feed per tooth of 0.085 mm/tooth. Conversely, the plasma-cut samples were prefabricated with 300A plasma and a cutting speed of 2.3 m/min. After the milling and cutting, the profile of the edges was measured in two directions, longitudinally and transversally, on two/three different sections of the surfaces. The results of average surface roughness measurements of both methods can be seen in Figure 1. The average measured surface parameters for milling and plasma cutting edges are the following: roughness of profile 1.84/ 3.64 μm (Ra), height of profile 4.66/ 12.14 μm (Rp) with waviness included, and mean peak to valley height of primary profile 8.68/ 20.67 μm (Rz), Figure 2. The results show that the milling method ensured higher edge quality than plasma cutting edges. Milled samples had a consistent quality across the entire cut surface, while a higher roughness with visible striations and irregularities characterizes the plasma-cut surface. Due to this, there is no zero-gap between the plasma-cut pieces, i.e., at the bottom, it is nearly 0 mm and opens slightly towards the top – similar to a V – groove joint preparation. The effect of surface quality on weld performance was rarely studied. According to Sokolov et al. [5], the particular range of surface roughness can significantly enhance penetration depth.

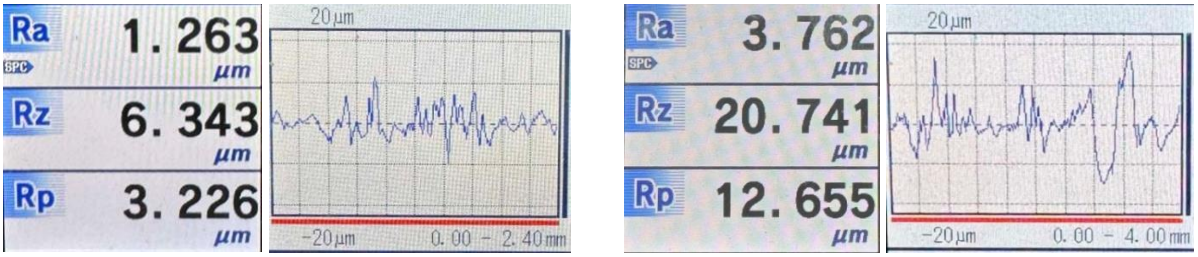

a) b)

Fig 2. Measured surface parameters for milling and plasma

Table 1 Chemical composition composition of the steel (%) according to mill certificate values

Material/element	C	Mn	P	S	Si	Cr	Ni	Mo	Cu	Fe
Base material S355J2	0.16	1.05	0.014	0.007	0.24	0.11	0.09	0.001	0.33	bal.
Filler material G3Ni1	0.078	1.46	0.012	0.012	0.85	0.014	0.73	0.08	0.10	bal.

Table 2 Mechanical properties of used materials

Material	Rp (MPa)	Rm (MPa)	A5 (%)	KV (J)
Base material S355J2	400	525	29.6	120 (-20 ºC)
Filler material G3Ni1	518 (min 470)	598 (min 560)	31 (min.26)	90 (-20 ºC)

2.3 Welding equipment and procedure

A high – power fiber laser IPG YLR-20000 of IPG was used in the experiments with the following parameters: an optical fiber with a 200 μm, beam parameter product of 11 mm×mrad, and 1070-nm wavelength. A laser processing head, BIMO HP, with a focal length of 350 mm providing a spot focus diameter (df) of 0.56 mm was used. A welding machine, Qineo Pulse 600 of Cloos, with a maximum current of 600 A was applied as a power source for the arc. GMAW was performed with a direct current of positive polarity (DC+).

The laser optics and GMAW torch were mounted on the robot arm, where the laser beam longitudinal inclination angle was 0° from normal towards the welding surface reflections, while the GMAW torch was tilted 65° to the welding surface, and the position of the robot remains unchanged during all welding process. The edge walls were cleaned with acetone to remove grease prior to welding. Before welding, edge surface roughness values and roughness patterns were measured transversely and longitudinally, and welds at the beginning and end of the plates were applied to ensure zero-gap and edge alignment. All the experiments were carried out with an arc-leading orientation and a distance of 3 mm

between the two heat sources. The focal position of the laser beam was − 3 mm relative to the workpiece surface. The wire stick-out was set to 15 mm. The HLAW process configuration is shown in Figure 3.

The experiment was conducted to achieve a weld without imperfections that will meet the standards EN ISO 12932 requirements with maximum possible productivity. Single-pass hybrid laser-arc welds were performed in a butt joint configuration with zero-gap by using the following process parameters, a laser beam power of 10 – 11.5 kW, welding speed 1.8 m min-1, welding current 355-390 A and arc voltage 36.8-38.2 V. Main parameters adjustment were the laser power and arc current, while the other process parameters were kept constant to simplify the study. The HLAW welding parameters can be found in Table 3.

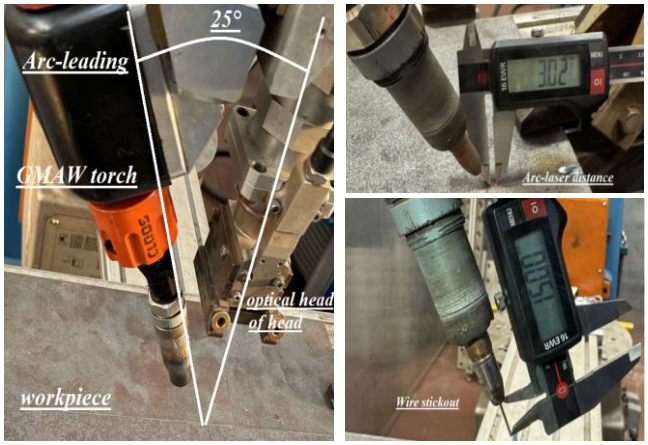

Fig. 3 HLAW system: a) experimental setup; b) heat sources distance; c) stick-out

Table 3 Single – pass welding process parameters

Weld no.	Methods of edge preparation	Gap (mm)	Laser Power (kW)	Arc mode	Arc current (A)	Arc voltage (V)	Wire feed (m/min)	Welding speed (m/min)	Focal position (mm)	Gas low rate (l/min)	Wire stick-out (mm)	Arc-laser distance (mm)
6	Milling	0	10	Pulse	389	38.2	14	1.8	-3*	25	15	3
11	Milling	0	10	Pulse	355	36.7	12	1.8	-3*	25	15	3
11-1	Milling	0	11.5	Pulse	359	36.8	12	1.8	-3*	25	15	3
20	Plasma-cut	0	10	Pulse	355	36.8	12	1.8	-3*	25	15	3

2.4 Testing

According to the standard EN ISO 15614-14 [6], destructive and non-destructive testing should be carried out after the welding process to determine the quality of welded pieces and their mechanical properties. A visual inspection in accordance with ISO 12932 is performed to detect surface defects such as undercutting, overlap, surface cracks, craters, and misalignment. In contrast, another non-destructive X-ray test is performed to detect internal weld defects. All HLAW welds were subjected to mechanical testing - tensile, bend and hardness testing.

The cross-weld tensile test, performed based on EN ISO 4136, uses the standard dimension and geometry of the tensile test specimen [7]. To ensure the most accurate results for the weld's tensile strength, non-standard tensile test specimens are created. These specimens feature a square notch in the weld from both sides, as shown in Figure 4 [8]. The purpose of this design is to provide a more comprehensive assessment of the weld's strength. The thickness of the test specimens matches the base material, without any machining of the root and face side of the weld.

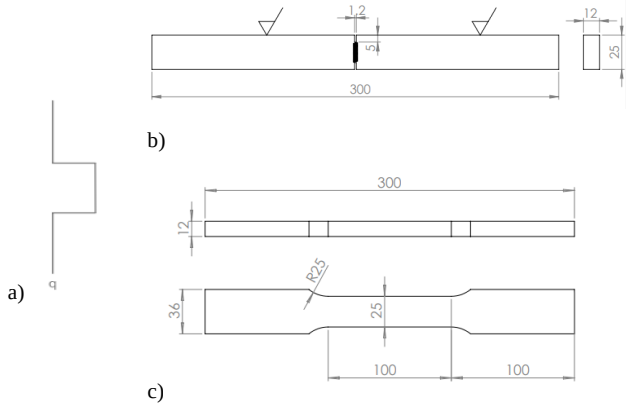

Fig. 4 a) square notch ISO 9017 [8]; b) non-standard tensile test specimens c) standard tensile test tensile

The bend test was performed according to EN ISO 5173 [16] based on transverse face side (FBB) and transverse root side bending of butt joint (RBB) subject to 180° angle bend, with the standard specimen dimension and geometry (12 x 30 x 300 mm^3). For testing, the former is used with a diameter (d)

30mm and distance between the rollers d+ 2ts + 1≤ l ≤ d + 3.5ts. The side of the former was milled prior to bending, while the other side was kept as welded so that any undercuts and underfills were included during testing.

Vickers hardness test (HV10) was performed in accordance with two standards, ISO 9015-1 [9] and ISO 22826 [10]; the first one was applied in the upper zone, the arc–laser zone, and the second one in the laser zone. The test specimens surface were polished and etched before testing, the measurements were performed in three rows of the material thickness: one below the weld face and one from the root side at a depth of <2mm, and one in the middle of the material thickness, figure 5 [10]. In each row, three areas were covered by three individual indentations, base material, heat-affected zone, and weld metal. The distance between the hardness indentations was set to 1 mm in the upper zone, and >3dv for the middle and root zone to avoid interferences between the results.

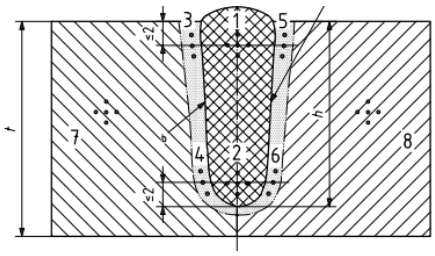

Fig. 5 Location of indentations in laser zone [10]

3. Results and discussion

The visual inspection of HLAW welds was found that three of four welded pieces can be classified in the highest evolution B in accordance with EN ISO 12932. The micrographs of the weld are shown in Figure 6, and in the Weld No. 11 can be noted root humping which is not acceptable according to ISO 12932 [17]. Humping in the root zone is the primary welding defect observed in the welding of milling sidewalls; the hump exceeds even the lowest quality level D: hump height = 1.0mm + 0.6 x width of the root. With an aim to suppress the humping in pieces with milling edge preparation, the laser beam power was increased to 11.5 kW, and the arc current was also increased to 390A. According to Bunaziv et al. [11] a slight air gap in the I-joint preparation can be beneficial to prevent humping by reducing the pressure in the keyhole. Therefore, using the same HLAW process parameters, zero-gap plasma-cut edges performed better because they can reduce the keyhole pressure due to the natural gaps formed by the peaks and valleys of the surface roughness. The striations of the plasma-cut can increase the laser absorption and, at the same time, improve the flow of molten filler material flow further inside the joint [3]. However, a larger air gap > 1mm will cause humping of the melt since the surface tension is not capable to sustain the dropout [11]. Another factor that influences the weld bead geometry and the humping process is the laser-arc power ratio. Due to this factor, using the same welding speed and getting a high-quality root without humping leads to a change in arc current weld no.6 and laser beam power in weld no. 11-1.

The micrographs of the weld and X–ray images show welds No. 6, 11-1 and 20 have no internal defects. In terms of weld bead, sample 20 is characterized by undercut, which size was acceptable with quality level B according to ISO 12932. Undercuts in arc welding are a consequence of the formation of a thin film of liquid metal that solidifies prematurely at the melt pool edges, hampering the liquid metal wettability and leading to cavities in these regions [12].

In terms of tensile strength, all weld pieces showed satisfactory results, even the Weld No. 11 with a root hump which is not acceptable from a visual point of view. All standard tensile test specimens exceeded the strength of the base material, reaching at least 385MPa yield strength and 560MPa ultimate tensile strength, resulting in BM failure, Figure 7a and d. Visual inspection may note elongation in the HAZ and a clear fusion line especially, in the laser–arc region after the tensile testing. Among the non-standard tensile test specimens with the square notch in the weld, the higher results

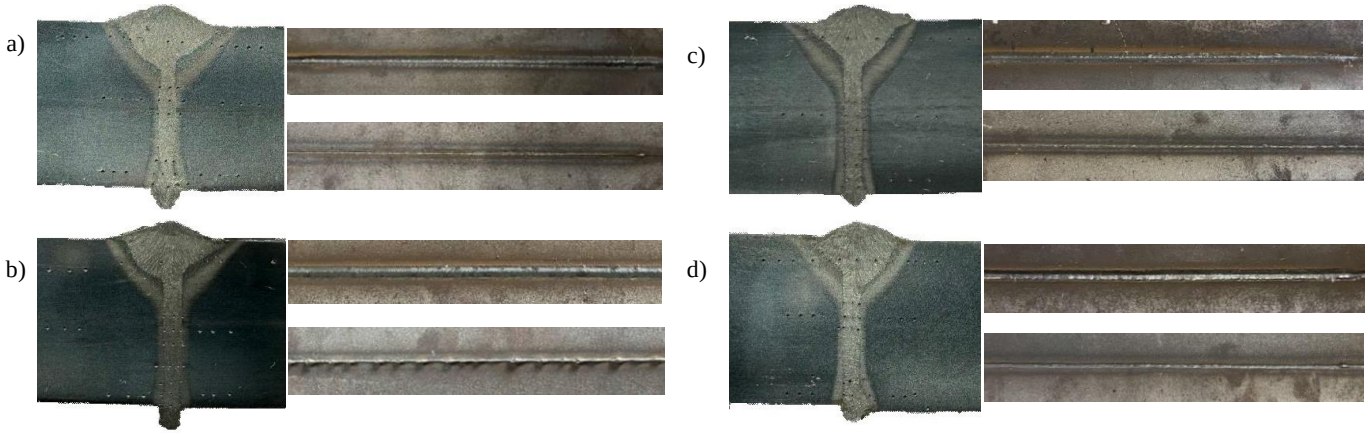

Fig. 6 Hybrid laser-arc weld of 12 mm thick plates: a) Weld No.6; b) Weld No.11; c) Weld No. 11-1; d) Weld No. 20

were achieved in Weld No.11-1, 556MPa yield strength and 689MPa ultimate tensile strength with a total elongation of 7.81%. Weld No.6 is characterized by the lowest weld strengths, 504MPa yield strength, and 636MPa ultimate tensile strength with a total elongation of 7.97%, Figure 7b.

Besides the stress concentration due to the square notch, all welds exceed the base material strength by at least 15%. The higher heat input in Weld No. 6, caused by the increased arc power, reduces the tensile strength. In general, the tensile strength is reduced with increasing heat input due to microstructure and the possibility of larger grains [11].

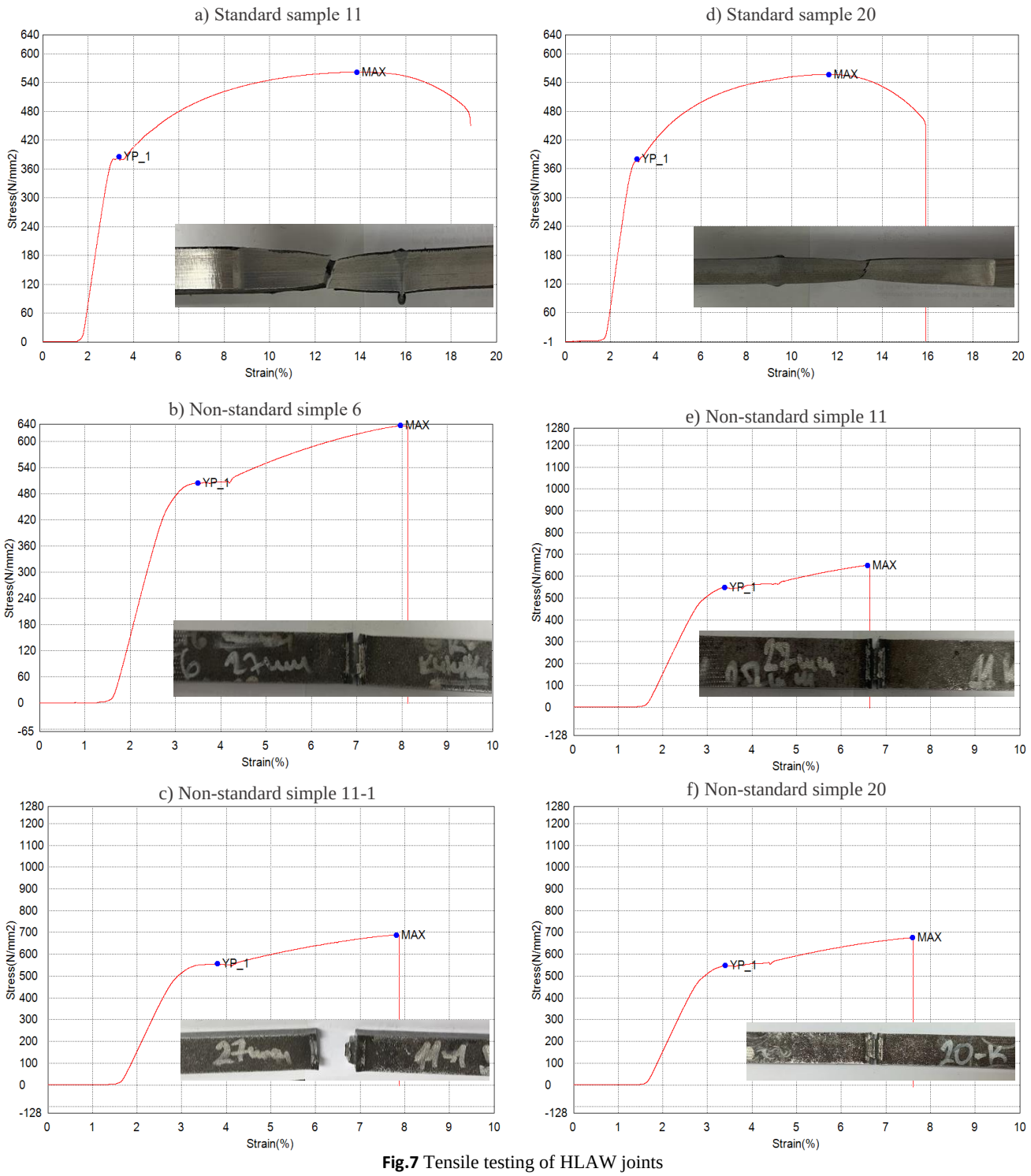

Fig.7 Tensile testing of HLAW joints

The qualitative results of the bend test are presented in Figure 8. A total of eight bend specimens were tested, two specimens of each welded piece, TFBB and TRBB. A bending angle of 180º was achieved in all TRBB bend specimens. On the other hand, one of four TFBB specimens reached the bend angle of 180º, while the other showed cracks in the fusion zone immediately after passing 120º, representing low ductility due to increased tensile strength and high cooling rates in the laser-arc region. Based on it, it is evident that heat produced by the arc flows from the laser-arc region to the laser region, increasing the cooling rates in the HAZ and producing less fusion in the upper zone. In Weld No.20, the natural V -groove in the upper zone provided better melt flow dynamics, leading to the most potent fusion in the arc-laser region. Bunaziv et al. [11] mentioned that the main disadvantage of plasma-cut edges is the frequent lack of fusion with sidewalls in the laser region, which can be related to uneven transversal geometry associated with slight deviation perpendicular to the plate surface. This type of imperfection was not found in the experiment.

The Vickers hardness HV10 values are presented in Figure 9. It can be seen that higher hardness values were found in the laser-arc region HAZ and the laser region FZ. For all the samples, the hardness values increased continuously from the base material to the fusion line in the laser region. In contrast, the hardness profile in the laser-arc region presented an M-shape with the highest hardness values in the HAZ. Welds with high tensile strength are expected to possess higher hardness. Therefore, average hardness values are compared between Weld No. 11-1 and 6. The average hardness values in the FZ and HAZ in the laser-arc region for Weld No.11-1 are 319 HV and 374 HV, while for Weld No.6 are 315 HV and 361 HV. In the middle row, the average hardness value in both zones reaches 320-330HV, below the maximum allowed hardness levels of 350HV accosting to standard ISO 15614-1 [13]. In the laser region, specifically in the HAZ of the root, the average hardness value is 390HV or 40HV above the permissible hardness level. However, this standard does not cover hybrid laser-arc welding. According to Wallerstein et al. [12], these hardness values are due to bainite and martensite microstructures in the HAZ. They can be eliminated by reducing the cooling rates, evident in Weld No. 6 by increasing the arc power, Figure 9a.

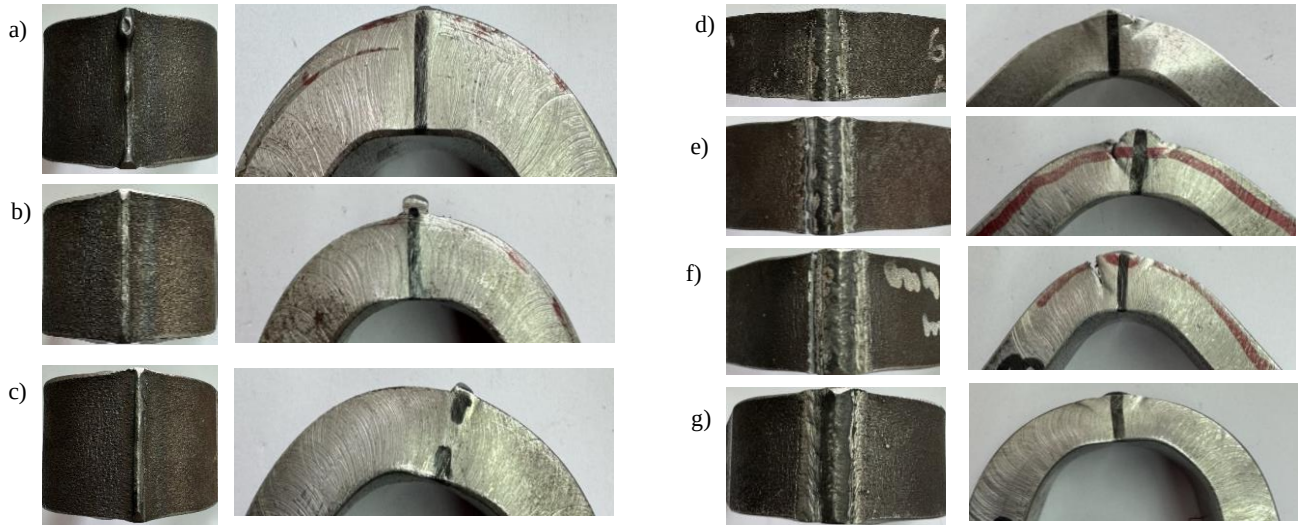

Fig. 8 Bending test results: TRBB a) 11, b) 11-1, c) 20; TFBB d) 6, e) 11, f) 11-1, g) 20

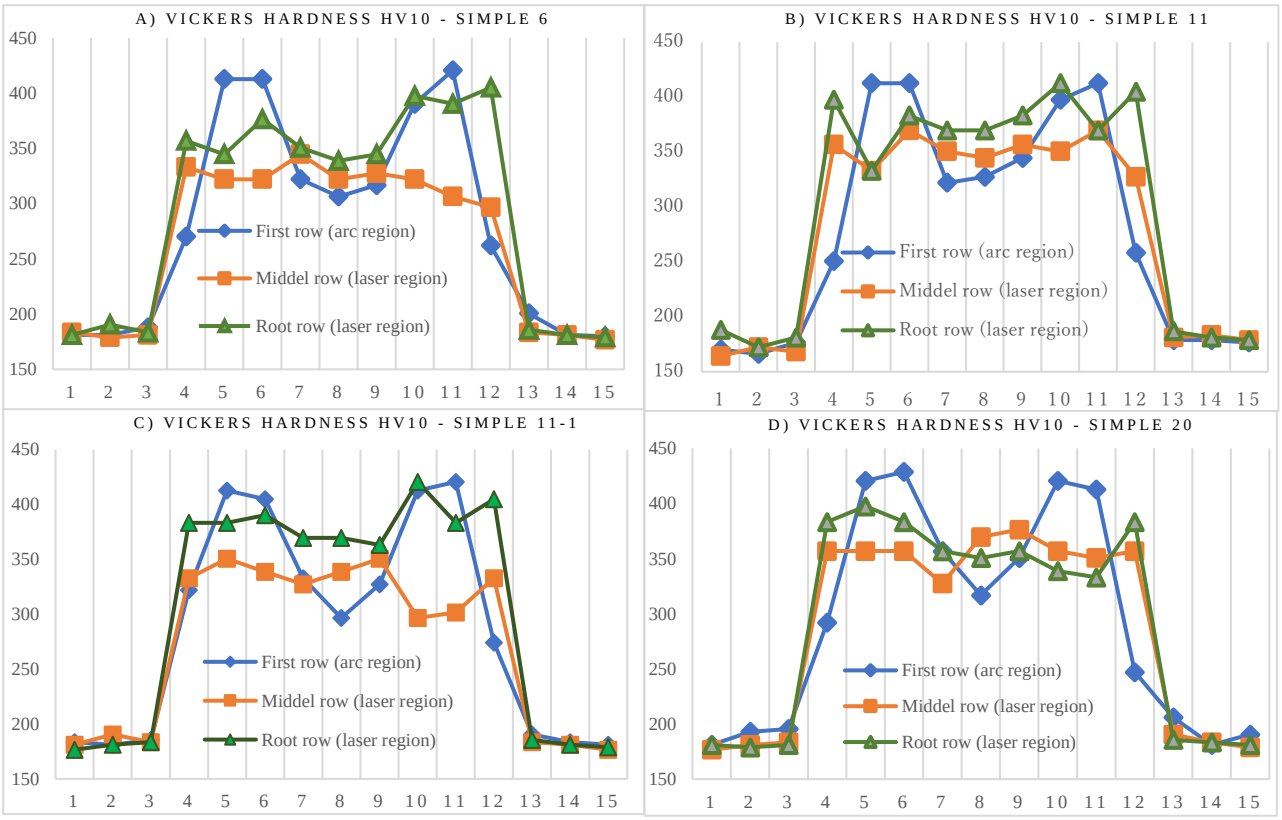

Fig.9 Results of Vickers hardness HV10

4. Conclusion

In this research, several experiments were conducted to evaluate the influence of edge surface quality on the single-pass hybrid laser-arc weld of 12-mm thick structural steel S355J2. Hybrid weld quality and its mechanical characteristics were discussed with respect to the industrial methods for edge preparation and the edge surface roughness. The most important conclusions from the present experimental results are the following:

- The slight air gap formed by the peaks and valleys of the surface roughness in the zero-gap joint of the plasma-cut piece prevents the humping due to improved melt flow dynamics and reduction of keyhole pressure. Plasma-cut edge surface preparation can be considered as an alternative industrial method to increase HLAW efficiency by using the same welding process parameters in an I-joint configuration with zero-gap.
- Among the milling sidewalls, the humping process can be eliminated by increasing the heat input and selecting the proper laser-arc power ratio. A high-quality hump-free root can be achieved with a higher arc power of 12.5% or with a laser power of 15%.
- The tensile strength of the hybrid welds exceeds the base material strength by at least 15% at the expense of ductility. Even a root hump weld that is not acceptable according to ISO 12932 can cover the strength of the base material. Based on the results, the hybrid welds are characterized with satisfactory strength.
- The edge surface quality can determine the selection of process parameter values and thereby indirectly influence the weld bead geometry. By increasing the arc power, the weld area in the arc-laser region increases, and vice versa.
- In terms of hardness, the highest hardness values were found in the HAZ of the laser-arc region and FZ of the laser region due to the high cooling rates. The averaged measured values in the laser region are 30-40HV above the permissible hardness level according to ISO 15614-1, but this standard does not cover hybrid laser-arc welding. By increasing the total line energy for HLAW, the hardness value would be decreased, which is evident in Weld no.6.

Reference

[1] Petreski, M., Runchev, D., and Vrtanoski, G.: *Hybrid laser arc welding – State of the art in technology. Welding and welded structures*, 66(3), (2021), pp 115-124.

[2] Farrokhi, F., Larsen, R.M., and Kristiansen, M.: *Single-pass hybrid laser welding of 25mm thick steel*. Physics Procedia 89, (2017), pp. 49-57.

[3] Farrokhi, F., and Kristiansen, M.: *A practical approach for increasing penetration in hybrid laser-arc welding of steel*. Physics Procedia 83, (2016), pp. 576-586.

[4] Farrokhi, F., Nielsen, S.E., Schmidt, R.H., Pedersen, S.S. and Kristiansen, M.: *Effect of cut quality on hybrid laser-arc welding of thick section steels.* Physics Procedia 78, (2015), pp. 65-73.

[5] Sokolov, M., Salminen, A., Somonov, V., and Kaplan, A.F.: *Laser welding of structural steels: Influence of the edge roughness level*. Optics and Laser Technology, 44(7), (2012), pp. 2064-2071.

[6] International Organization for Standardization: *EN ISO 15614-14:2013 Specification and qualification of welding procedures for metallic materials — Welding procedure test — Part 14: Laser-arc hybrid welding of steels, nickel and nickel alloys*. ISO, (2013).

[7] International Organization for Standardization: *EN ISO 4136:2012 Destructive tests on welds in metallic materials — Transverse tensile test*. ISO, (2012).

[8] International Organization for Standardization: *ISO 9017:2017 Destructive tests on welds in metallic materials — Fracture test*. ISO, (2017).

[9] International Organization for Standardization: *ISO 9015-1:2013 Destructive tests on welds in metallic materials — Hardness testing — Part 1: Hardness test on arc welded joints*. ISO, (2013).

[10] International Organization for Standardization: *ISO 22826:2013 Destructive tests on welds in metallic materials — Hardness testing of narrow joints welded by laser and electron beam (Vickers and Knoop hardness tests*. ISO, (2013).

[11] Bunaziv, I., Dørum, C., Nielsen, S.E., Suikkanen, P., Ren, X., Nyhus, B., Eriksson, M., and Akselsen, O.M.: *Laser-arc hybrid welding of 12-and 15-mm thick structural steel*. International Journal of Advanced Manufacturing Technology, 107, (2020), pp. 2649-2669.

[12] Wallerstein D., Vaamonde E., Prada A., Torres, E.A., Urtiga Filho, S.L., and Santos, T.F.A (2020) *Influence of welding gases and filler metals on hybrid laser- GMAW and Laser-FCAW welds.* Mechanical Engineering Science 0(0), p.3-14.

[13] International Organization for Standardization: *ISO 15614-1:2017 Specification and qualification of welding procedures for metallic materials — Welding procedure test — Part 1: Arc and gas welding of steels and arc welding of nickel and nickel alloys*. ISO, (2017).

[14] Ustundag, O., Gook, S., Gumenyuk, A., and Rethmeier, M.: *Mechanical Properties of single-pass Hybrid laser arc welded 25mm thick-walled structures made of fine-grained structural steel*. Procedia Manufacturing 36, (2019), pp. 112-120.

[15] Sokolov, M., Salminen, A., Katayama, S., and Kawahito, Y.: *Reduced pressure laser welding of thick section structural steel*. Journal of Materials Processing Technology, 219, (2015), pp. 278-285.

[16] International Organization for Standardization: *EN ISO 5173:2023 Destructive tests on welds in metallic materials — Bend tests*. ISO, (2023).

[17] International Organization for Standardization: *ISO 12932:2013 Destructive tests on welds in metallic materials — Microhardness testing of welds*. ISO, (2013).

International Institute of Welding
Join to the Future

Doc. IV-1598-2024

Annual Assembly Dodecanisa, Rhodes, Greece 2024

Venue: Rodos Palace Hotel, Trianton Avenue, Ixia 85100

Preliminary Agenda

C-IV: Power Beam Processes
8-10 July 2024
Room: Listed by day of meeting
Chair: Dr. Patrick Hochanadel (USA)

Monday 8 July 2024, 0900-1300 - Nafsika B

1. Opening of the Meeting
2. Request Meeting Secretary to write the Minutes of Meeting
3. Attendees and Apologies, Identification of C-IV delegates
4. Approval of the minutes from the last annual assembly in Singapore (Doc. IV-1588-2023)
5. Adoption and Agreement of Agenda (Doc. IV-1598-2024)
6. Discussion of Joint Intermediate Meeting in Cambridge, UK
7. Presentation of documents

0920 Session 1: C-IV Papers (20 minutes per paper including questions)

[01] 0905: Electron Beam Welding of 2205 Duplex Stainless Steel for Safety Critical Components
D. Holiver, B. Holmes, C. Punshon, S. Smart, and E. Broughton (United Kingdom)
IV-1609-2024

[02] 0925: Life Cycle Assessment in Additive Manufacturing of Copper Alloys – Comparison between Laser and Electron Beam
J. Raute, A. Beret, M. Biegler, and M. Rethmeier (Germany)
IV-1610-2024

[03] 0945: Electron Beam Welding of Motor Stator Wire for Mass Production Environments
A. Ofarrell, D. Chantzis, M. Higgins, W. Dunn, and C. Guest (United Kingdom)
IV-1612-2024

[04] 1005: Electron Beam Welding of Battery Packs
C. Ribton, V. Jefimovs, and D. Holiver (United Kingdom)
IV-1611-2024

[05] 1025: Factors Affecting Quality and Properties of Local Vacuum Power beam Welds in Energy Application
C. Punshon (United Kingdom)
IV-1613-2024

1045-1115: Coffee break

1115 Session 2: C-IV Papers (20 minutes per paper including questions)

[06] 1120: Laser Beam Welding in Vacuum for Additive Manufactured Parts – Development of a multilayer vacuum insulated hydrogen cryogenic tank
B. Gerhards, P. Stockem, J. Bührung, S. Leuders, F. Eichler, and S. Bremen (Germany)
IV-1615-2024

[07] 1140: Quantifying and Evaluating Efficacy of Window Protection Systems in Laser in Vacuum Welding
M. Nentwich (United Kingdom)
IV-1616-2024

[08] 1200: In-Situ Monitoring and Online Prediction on Keyhole Penetration In Robotic Arm Laser Welding Using Melt Pool Images
H.H.L. Núñez, L.-W. Hsu, K.S.B Ribeiro, W.M. Bessa, and A. Salminen (Finland)
IV-1617-2024

[09] 1220: Impact Of Beam Oscillation and Power Modulation on The Intermixing Behavior of Dissimilar Titanium / Niobium / Nitinol Joints during Micro Electron Beam Welding
M. Wiegand, M. Kahlmeyer, W. Song, and S. Böhm (Germany)
IV-1618-2024

[10] 1240: Prediction of Porosity Formation in High-Power Laser Beam Welding using Physics-Informed Machine Learning Framework
X. Meng, M. Bachmann, K. Pascal, M. Rethmeier (Germany)
IV-1614-2024

Close of Day 1 Activities

Tuesday 9 July 2024, 0855 -1830 @ Delphoi
Joint Meeting of C-I, C-IV, and C-XII

Morning Session, 0855-1300
Session 1, Chair: Professor Satoru Asai

0855: Opening of Joint Meeting of C-I, C-IV, and C-XII – Professor Satoru Asai

[11] 0855 3D Printing and Surfacing of Inconel 625 through Automated Wire Arc Additive Manufacturing
C. Goulas, M.J.M. Hermans, A. Rajes, R. Rook, B.E. Satiti, H. Thompson, W. Ya (Netherlands)
Doc. XII-2706-2024/I-1616-2024/IV-1647-2024

[12] 0915: A Heat Source for Milliscale WAAM Technology
S. Shigematsu, H. Komen, M. Tanaka, T. Murata, A. Murata (Japan)
Doc. XII-2696-2024/I-1617-2024/IV-1648-2024

[13] 0935: Mitigation of Ductility Dip Cracking in Invar 36 Alloy during Wire Arc Additive Manufacturing through Enhanced Cooling and *in-situ* Alloying of TiC Particles
C. Goulas, M. Herman, V. Popovich, A. Sood (Netherlands)
Doc. XII- 2687-2024 /I-1618-2024/IV-1649-2024

[14] 0955 Forming Regulation in Additive Manufacturing based on a Novel Model: In-order Stacking of Primitives
S. Chen, J. Xiao, Z. Yan (China)
Doc. XII- 2685-2024 /I-1619-2024/IV-1651-2024

[15]1015: Feasibility Study on Machine Learning Methods for the Prediction of Process Parameters for the WAAM Process using SS-316L Filler Material
A.H. Reise , P.S. Sharath, S. Sheikhi (Germany)
Doc. XII- 2682-2024 /I-1620-2024/IV-1650-2024

Presentation by IIW Staff/Elisabetta Sciaccaluga (IIW)

Coffee Break (1045– 1115)

Session 2, Chair: Professor Satoru Asai

[16] 1115: Combination of the Melt Pool Gometry Parameters with the Audio Data for Defect Detection in GMAW and WAAM
D. Havrylov (Canada)
Doc. XII-X 2684-2024 /I-1621-2024/IV-1652-2024

[17] 1135: Influence of Edge Surface Quality on Hybrid Laser Arc Welding of Structural Steel S355J2
M. Petreski, D. Runchev, G. Vrtanoski, A. Krstevska (North Macedonia)
Doc. XII- 2668-2024 /I-1622-2024/IV-1653-2024

[18] 1155: Application of Tailor Welded Blanks to Rudder Frame Using Laser-Arc Hybrid Welding
T. Era, K. Takeda, T. Egawa, K. Kashiwabara, M. Tatsutomi, H. Uchiyama (Japan)
Doc. XII- 2689-2024 /I-1623-2024/IV-1654-2024

[19] 1215: Investigating the Effect of Shielding Gas on Arc Plasma Behaviors and Welded Quality in GMAW-GTAW Hybrid Welding Process on AA5083 Aluminium Alloy
T. Methong, R. Boonrungsee, B. Chanprasertkul (Thailand)
Doc. XII- 2666-2024 /I-1624-2024/IV-1655-2024

[20] 1235: Effect of Current Waveform in MIG Arc on Weld Bead Formation in Plasma-MIG Hybrid Welding
S. Tashiro, K. Ishida, K. Nomura, D. Wu, A.B. Murphy, T. Yuji, M. Tanaka (Japan)
Doc. XII- 2701-2024 /I-1625-2024/IV-1656-2024

Afternoon Session, 1425-1830
Session 3, Chair: Dr. Patrick Hochanadel

1425: Opening of Afternoon Session of C-I, C-IV, and C-XII – Dr. Patrick Hochanadel

[21] 1425: Effect of Welding Speed on Keyhole Behavior and Spatter Formation in Full Penetration Laser Beam Welding using High-Speed Synchrotron X-Ray Imaging
C. Diegel, K. Schricker, L. Schmidt, M. Seibold, H. Friedmann, P. Hellwig, F. Fröhlich, J.P. Bergmann, F. Nagel, P. Kallage, A. Rack, H. Requardt, and Y. Chen (Germany)
Doc. XII-2711-2024/I-1626-2024/IV-1619-2024